



## **A TWIN-CATHODE DC ARC SMELTING TEST AT MINTEK TO DEMONSTRATE THE FEASIBILITY OF SMELTING FeNi FROM CALCINE PREPARED FROM SILICEOUS LATERITE ORES FROM KAZAKHSTAN FOR ORIEL RESOURCES PLC**

**I.J. Reinecke and H. Lagendijk**

*Council for Mineral Technology, 200 Hans Strijdom Drive, Randburg, South Africa  
E-mail: isabelr@mintek.co.za, hermanl@mintek.co.za*

### **ABSTRACT**

*Mintek was contracted by Oriel Resources plc in 2004 to conduct a preliminary assessment study on smelting ferronickel from the large but relatively low grade Shevchenko nickel ore deposit in Kazakhstan.*

*A detailed feasibility study (“DFS”) was awarded to Bateman BV following promising results from the preliminary assessment study (“PAS”) and small-scale pilot plant test work. As part of the DFS, a total of 450 metric tons of ore was collected from three different locations in the deposit and shipped to Mintek. After sampling, the bulk sample was prepared for smelting. This comprised crushing, screening and calcining with each step done separately for the three different lots.*

*The chemical composition of the ore from the deposit is relatively high in silica and therefore falls out of the MgO to SiO<sub>2</sub> range that is normally processed by pyrometallurgical means to produce ferronickel. The main objective of the testwork was to demonstrate that a method could be found and successfully applied to smelt these siliceous ores and produce an acceptable nickel-containing alloy.*

*A 2-m ID DC arc furnace was installed with a twin-cathode (electrode) configuration to replicate the proposed commercial-scale furnace and also incorporated an advanced design of water-cooled copper panels in the lower furnace sidewalls to withstand the aggressive nature of the high SiO<sub>2</sub>-containing slags.*

*The reductant used was a high-volatile coal from Karaganda in Kazakhstan. The reductant addition was adjusted to achieve a 90% recovery of nickel. In the assessment of the process metallurgy, some deviation from equilibrium conditions was observed. This deviation is ascribed to the intermittent existence of a smelting bath partially covered with feed during the testwork. Optimization of smelting conditions should result in the metallurgy (slag metal equilibrium) being closer to the theoretical predictions and make the production of a 20% nickel alloy possible at 90% nickel recovery.*

*The solution for the successful processing of these siliceous ores was found in the attainment of the necessary operational stability through the control of arc length, operating temperature, open-bath smelting conditions and flux additions of up to 10% dolime for the most siliceous of the three ore types. The test work carried out by Mintek provided the basis for the process flow sheet and engineering design of the DC arc smelting furnaces for the Shevchenko Nickel project.*

### **1. INTRODUCTION**

Production of nickel from laterite (oxide nickel ores) has been practiced for over 100 years starting with the processing of laterite ores in New Caledonia in the late nineteenth century. Since the discovery of sulphide deposits in the Sudbury area early in the twentieth century, the processing of nickel has been predominantly from these ore types[1].

The importance of laterites has, however been growing during the twentieth century from less than 10% in the 1950's to over 40% at the turn of the century and is predicted to account for over 50% of primary nickel production after about 2010[2].

Although the processing of sulphide deposits has been dominant, the nickel contained in laterite deposits account for over 70 % of land-based resources, roughly 40 % of which would be suitable for processing by pyrometallurgical methods[2].

Oxide nickel ores are processed either hydrometallurgically or pyrometallurgically. Usually the high-magnesia type ores, denominated as saprolitic laterite, (which typically contain lower cobalt and iron than limonitic type ores, are processed using pyrometallurgy. The nickel-to-cobalt ratio is generally of the order of 40:1. In hydrometallurgy, the Caron Process or HPAL (high pressure acid leaching) is typically used to recover both nickel and cobalt. For HPAL, the combined magnesia and alumina content should preferably be lower than about 5% to prevent excessive consumption of acid. The Caron process, on the other hand, is actually a combined pyrometallurgical and hydrometallurgical process where the first steps include drying, calcining and reduction at about 700°C. The metallics are then extracted by leaching with ammonia solution. The nickel recoveries are lower than with smelting or HPAL, and the cobalt recoveries are lower than with HPAL. Ullman's Encyclopedia[3] gives broad guidelines as to whether a specific ore type is suitable for pyrometallurgical or hydrometallurgical processing. The summary of the guidelines are given in Table 1 below:

**Table 1: Guidelines with respect to the processing techniques for laterite ores, based on chemical composition**

Description	Approximate assays on dry ore basis, %					Extractive procedure
	Ni	Co	Fe	Cr <sub>2</sub> O <sub>3</sub>	MgO	
Hematitic overburden	<0.8	<0.1	>50	>1	<0.5	Removed to stockpile
Limonite	0.8 to 1.5	0.1 to 0.2	40 to 50	2 to 5	0.5 to 5	Hydrometallurgy
'Transition' material	1.5 to 1.8	0.02 to 0.1	25 to 40	1 to 2	5 to 15	Hydrometallurgy or Pyrometallurgy
Altered peridotite – 'silicate nickel ores / garnierite/saprolite / serpentine'	1.8 to 3		10 to 25		15 to 35	Pyrometallurgy
Unaltered peridotite 'silica bedrock'	0.25	0.01 to 0.02	5	0.2 to 1	35 to 45	Left in situ

The first part of the study for Oriel Resources on the siliceous ore from Kazakhstan comprised an assessment as to the most appropriate processing technology. Laterites typically comprise mainly the chemical compounds SiO<sub>2</sub>, Fe<sub>2</sub>O<sub>3</sub> and MgO. These three compounds make up roughly 94 ± 3% of the total ore on a calcined basis, where calcining removes free and crystalline water to a residual LOI (loss on ignition) of less than 1 %. The remainder of the chemical species are primarily Al<sub>2</sub>O<sub>3</sub>, Cr<sub>2</sub>O<sub>3</sub> and Mn<sub>2</sub>O<sub>3</sub>.

In Figure 1 underneath, the position of the ore compositions of samples from several locations in the deposit, denominated as S, B, and T, are compared with those of other ores used in industrial laterite smelters, using a ternary SiO<sub>2</sub>-MgO-Fe<sub>2</sub>O<sub>3</sub> phase diagram[4]. Data from industrial smelters were derived from different smelter surveys[5],[6],[7], with the feed compositions given on a dry ore basis and normalized to the above-mentioned three main compounds. The compositions of some ores used in processing by HPAL and in the Caron process are also shown for comparison. For the HPAL process, ore feed information from the Bulong, Cawse, Murrin Murrin and Moa Bay operations were used[8]. Data from the ores used at Nicaro and Punta-Gorda, both of which employ the Caron process, were also obtained[9], but because of the similarity in the latter two ore compositions, they present only one data point on the diagram. In addition, the compositions of the fluxed ore samples are indicated on the phase diagram, with the basic oxide CaO combined with MgO and represented as MgO on the ternary phase diagram.

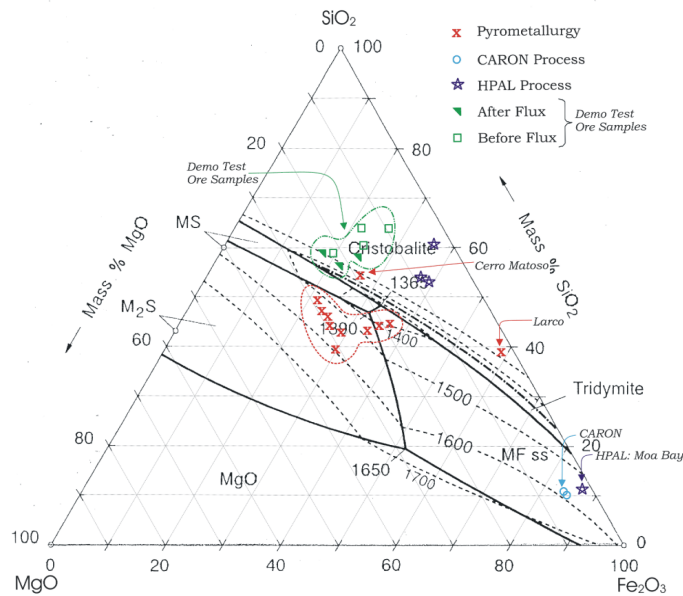


Figure 1: Ternary phase diagram showing the composition of the Kazakhstan ore samples relative to industrial nickel ores processed by RK-EF smelting, PAL and the Caron process

It can be seen that most industrial laterite smelters process ores where the SiO<sub>2</sub>-to-MgO ratio is between 1 and 3, with the only exception being the Larco operation. The chemical composition of the ores from the deposit under investigation falls out of the SiO<sub>2</sub>-to-MgO range that is normally processed to produce ferronickel. The only reference to an ore type that was smelted in a electric furnace that resembles that of the sample under investigation, is that of the former operation in Kosova, which closed down in 1984 due to war in the region[10]. As such, these ore samples presented a new challenge, and the main objective of the testwork was to demonstrate that a pyrometallurgical method could be found and successfully applied to smelt these siliceous ores and produce an acceptable nickel-containing alloy.

Figure 2 shows the slag compositions derived from the smelting of the ore samples on a ternary SiO<sub>2</sub>-MgO-FeO phase diagram to differentiate the slag compositions resulting from the smelting of these ore samples against those slags produced during the smelting of more common pyrometallurgical laterite ores. The amount of CaO has been added to the amount of MgO to show the combined effect of fluxing with dolime, and shown on the SiO<sub>2</sub>-MgO-FeO, assuming that the behaviour of CaO and MgO would not be all that different. Also, the effect of about 5% minor components (Al<sub>2</sub>O<sub>3</sub>, Cr<sub>2</sub>O<sub>3</sub>, and Mn<sub>2</sub>O<sub>3</sub>) is likely to reduce liquidus isotherms as shown by 30 to 70°C.

## 2.DEMONSTRATION-SCALE TESTWORK

A detailed feasibility study (DFS) was awarded to Bateman BV following promising results from the preliminary assessment study (PAS) and small-scale pilot-plant testwork. The DFS required that the selected process be convincingly demonstrated by means of large-scale smelting testwork.

The high MgO content of the limonite phase and the variability of the distribution of the mineral phases making selective mining difficult excluded the use of conventional hydrometallurgical processes. Several new hydrometallurgical approaches were considered by Oriel Resources but it was decided that these were not well enough developed to exploit for the Shevchenko project and that a pyrometallurgical process should be pursued.



mittently with nickel content of up to 22%. A small addition of a MgO-based flux was found to have beneficial effects on the recovery of nickel.

A larger scale smelting test was then initiated with the objective of attaining a 90% nickel recovery and producing a 20% nickel grade under similar conditions to the envisaged commercial furnace.

### 2.1 Ore Sample Preparation

As part of the DFS, a total of 450 metric tons of ore was collected from three different locations in the deposit and shipped to Mintek. After ROM (Run-of-mine) sampling, the bulk sample was prepared for smelting. This comprised crushing, screening, homogenization, and calcining with each step done separately for each of the three lots.

The summary chemical analyses of the calcined ore samples are given in Table 2. Also included is material 'P', that was product material produced elsewhere during flash calcining testwork on the Kazakhstan ores. This material was sized at -1mm, whereas the main three samples were sized at -6mm. The 'P' material was about 15 tons and was destined to be smelted initially during the 'warm-up' stage of the demonstration test.

All the calcine samples with the exception of 'B', had flux added to them to counter the high silica content of the ore. Based on the flux addition, the 'calcine' composition was recalculated to include the effect of the flux, and enable plotting the composition of 'fluxed calcine' on the ternary SiO<sub>2</sub>-MgO-FeO phase diagram shown in Figure 1. The fluxed calcine analyses are given in Table 3.

**Table 2: Chemical composition of the calcined ores smelted during the demonstration test**

Ore type	Chemical composition of calcine, mass %								
	NiO	CoO	Fe <sub>2</sub> O <sub>3</sub>	SiO <sub>2</sub>	MgO	CaO	S	P	LOI
P	1.86	0.12	21.2	55.3	10.9	3.6	0.024	0.018	1.5
S	2.03	0.27	23.8	57.5	8.1	0.7	0.037	0.070	2.0
T	1.25	0.05	18.7	58.1	11.8	0.8	0.017	0.012	4.3
B	1.59	0.05	16.2	52.6	17.3	2.3	0.038	0.093	5.5

LOI: Loss on Ignition.

**Table 3: Chemical composition of the 'fluxed calcined' ores smelted during the demonstration test**

Ore type	Chemical composition of calcine, mass %								
	NiO	CoO	Fe <sub>2</sub> O <sub>3</sub>	SiO <sub>2</sub>	MgO	CaO	S	P	LOI
P + D	1.75	0.11	20.0	52.1	12.6	7.0	0.023	0.019	1.4
S + D	1.84	0.25	21.8	52.4	10.7	5.6	0.034	0.067	1.8
T + D	1.15	0.05	17.4	53.8	13.9	5.3	0.016	0.014	4.3

### 2.2 Reductants and Flux

Two different types of reductant were used, namely a high-volatile coal from Karaganda in Kazakhstan, and a local South African bituminous coal. The Karaganda coal was crushed and screened to +2 – 10mm, and was used in the smelting of the P, S, and T samples. The South African coal was sized at -15mm and used in the smelting of the B sample. The proximate analyses of the two reductants (in mass %) are shown in Table 4.

**Table 4: Proximate analyses of reductants used in the smelting testwork**

Reductant type	Karaganda coal	SA bituminous coal
Fixed carbon	44.7	61.4
Ash	9.8	15.3
Volatiles	38.9	22.1
Moisture	6.6	1.1
Sulphur	0.33	0.31
Phosphorous	0.080	0.085

The flux that was used was dolime (calcined dolomite) with 37% MgO and 55% CaO, denominated as 'D' in the above table.

### 2.3 Demonstration Plant Setup

The plant consisted of a feed system, furnace and offgas treatment train. The feed system was split such that the calcine, reductant and dolime flux could be fed from three dedicated feeders into a common downpipe such that all feed materials entered at a single entry port in the conical roof of the furnace. The three separate feeders enabled instantaneous smelting recipe adjustment if and when required. Figures 3 and 4 show a general photograph of the furnace and a 3D drawing of the furnace shell with the watercooled copper panel installation respectively.

Figure 5 shows a sketch of the refractory installation in the hearth and in front of the copper cooling panels as well as the relative heights of the metal and slag tapholes. Figure 6 shows a drawing of the twin cathode arrangement. The offgas train consisted of a combustion chamber where the CO offgas was combusted to CO<sub>2</sub> before being cleaned in a baghouse and discharged to atmosphere via a stack. Dust collection was done at a



Figure 3: General view of furnace

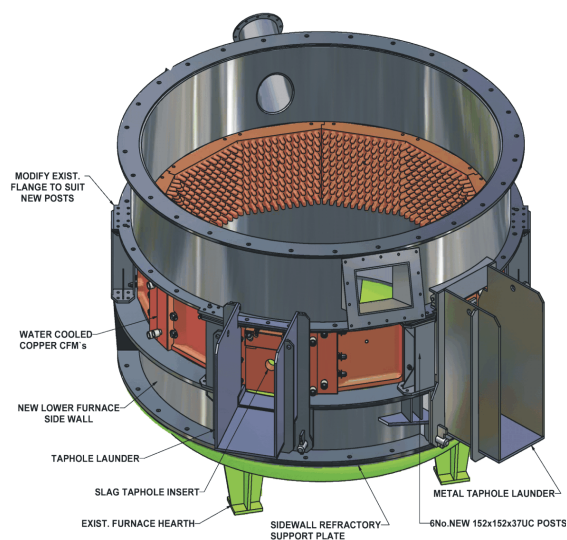


Figure 4: 3D view of furnace shell with water cooled panels

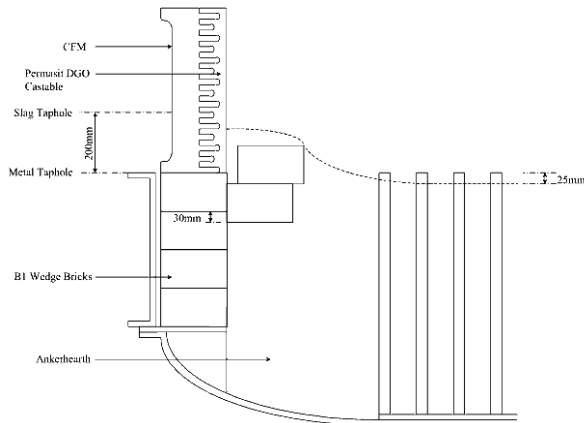


Figure 5: Sketch showing furnace refractories and taphole positions

high-temperature alarm limit in the watercooled copper panels. Slag was tapped intermittently when a batch had been fed and metal tapping operations were performed when temperatures in the control thermocouples of the watercooled panels started to approach alarm levels. The frequency of metal tapping operations corresponded roughly with every 5<sup>th</sup> slag tapping operation or every 6 tons of calcine fed. There were 162 slag tapping operations and 33 metal tapping operations in total. Carry-over dust was collected intermittently from the combustion chamber dropout box and the bagplant discharge respectively. The proportioning of the dust carry-over was roughly 25% to the dropout box and the remainder (75%) to the baghouse discharge.

combustion chamber ‘drop-out box’ and also at the baghouse.

### 2.4 Demonstration Plant Operation

The feed materials were blended in the desired ratio and fed at ambient temperature as 1.2-ton calcine batches (on average) at a predetermined feedrate through a single feedport into the furnace. The furnace feedrate was maintained at a level dictated by the power-to-feed ratio balance that was required to facilitate a specific operating temperature. The instantaneous smelting rate varied between 700 and 1400 kg/h during the various smelting conditions at corresponding power levels of 1 to 1.8 MW. The mode was closer to 850 kg/h at power level of about 1300 kW. The lower than planned feedrate was dictated by a power level limit of 420 kW/m<sup>2</sup> hearth area which coincided with a

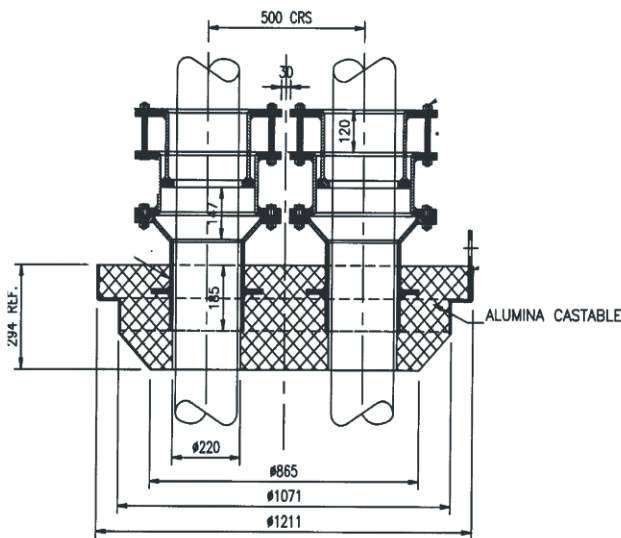


Figure 6: Drawing of twin-cathode configuration

Samples were taken from the slag and metal tapping streams respectively and submitted for quick turn-around chemical assaying. Metallurgical decisions were made primarily on the slag assays that were received back. Based on these the nickel recovery and reduction of iron could be established and changes to reductant addition implemented to achieve the primary target of nickel recovery to exceed 90%.

The electrical side of the furnace operation was controlled by a voltage setpoint for each of the two cathodes. This setpoint was set at between 370 and 430 V to achieve open arc operation. The PLC controlled the movement of the electrodes up and down to achieve the voltage setpoints. One of the arcs was prone to higher instability due to its proximity to the feed entry point, and the automated control was sometimes too slow to prevent the arc from extinguishing. For this reason, this electrode was

frequently operated in a manual mode where an operator would be manually raising and lowering the cathode to maintain maximum voltage but not 'losing the arc'.

### 2.5 Demonstration Plant Smelting Campaign Overview

The demonstration smelting campaign was conducted over a period of approximately five weeks with seven distinct periods/events. The chronology of these is summarized in Table 5.

**Table 5: Chronology of events during smelting campaign**

No.	Duration	Period/event
1	7 days	Furnace warm-up using propane gas, commissioning water-cooling circuits and feed system
2	8 days	Electrical warm-up on 0.5 ton scrap metal, feeding/smelting 15 tons of 'P' calcine
3	2 days	Completed first metal tapping operation, switched to 'S' material and raised furnace inventory. This resulted in foaming incident, incurring downtime due to required cleanup of material (slag) in the feedpipes
4	8 days	Smelting of 'S' material – 78 tons thereof
5	2 days	Attempt to feed 'B' material through preheating kiln – hot feed system. Resultant blockages in the feed system necessitated a switch to a belt feeder system, albeit that calcine had to be fed at ambient temperature – about 5 tons 'B' processed, before switching to 'T' material
6	5 days	Smelting of 'T' material – 63 tons thereof
7	3 days	Smelting of 'B' material – 32 tons thereof

The mass balance for the smelting campaign is given in Table 6.

**Table 6: Summary of feed ad product masses**

Feed materials, ton		Products, ton	
Feed material type	Mass, tons	Product type	Mass, ton
'P' calcine	14.7	Discard slag	180.5
'S' calcine	77.8	Alloy	11.8
'B' calcine	37.2	Bagplant dust	4.4
Karaganda coal	10.1	Drop-out box dust	1.6
SA coal	2.3		
Dolime flux ('D')	14.1		
Electrode consumed	1.5		
Start up scrap metal	0.5		
TOTAL	221.5	TOTAL	198.3

Due to the viscous slag tapped when the change-over from 'P' calcine to 'S' calcine was made with the consequent risk of further slag foaming, the flux addition was increased from 7% to 10% after about 16 tons of 'S' material had been processed. The rest of the condition was utilized to get stable smelting conditions and to increase the operating temperature (by increasing power-to-feed ratio) to eventually smelt consistently around 1675°C. In both the 'T' and 'B' smelting conditions, the reductant addition was the variable and increased to finally meet the target of >90% nickel recovery. Condition 'B' utilized SA coal and no flux was used.

### 3. DEMONSTRATION-SCALE TESTWORK RESULTS

#### 3.1 Stable Smelting Conditions

Stable operating conditions were selected within the overall smelting of the ‘S’, ‘T’, and ‘B’ materials and the key operating parameters are summarized as follows:

**Table 7: Key parameters during stable smelting of ‘S’ and ‘T’ and ‘B’ calcine**

Key parameter	Calcine ‘S’	Calcine ‘T’	Calcine ‘B’
Average total power input, MW	1.32	1.32	1.32
Average total power flux, kW/m <sup>2</sup> hearth area	420	420	420
Average instantaneous feedrate, kg/h	800	710	730
Average instantaneous smelting rate, kW/h.m <sup>2</sup> hearth area	255	225	230
Average carbon (in reductant) addition, kg/ton calcine	25	41	48
Average flux addition, kg/ton calcine	100	91	0
Average slag tapping temperature, °C	1680	1690	1725
Total calcine fed during selected period, t	15.8	16.4	18.2
Total reductant fed during selected period, t	0.9	1.5	1.4
Total dolime fed during selected period, t	1.6	1.5	0
Total crude ferronickel tapped during selected period, t	1.1	1.4	1.2
Total slag tapped during selected period, t	15.1	14.6	14.7
Average nickel in discard slag during selected period, mass %	0.18	0.10	0.14
Average FeO in discard slag during selected period, mass %	15.6	11.1	9.8
Average nickel in alloy tapped during selected period, mass %	20.1	16.5	15.6
Number of crude ferronickel alloy taps within selected period	3	5	5
Average cobalt in alloy tapped during selected period, mass %	2.3	0.9	0.6
Nickel recovery calculated based on nickel losses to slag, %	89	91	91
Crude alloy nickel grade calculated based on slag analyses, %	21.4	13.8	17.4

The nickel recovery reported in the previous table was calculated using the formula:

$$R_{Ni} = (Ni_{feed} - Ni_{slag}) / (Ni_{feed})$$

The nickel losses to the offgas train was ignored in the recovery calculation based on the assumption that these losses would be recycled to the furnace. Total dust losses were 3% of the calcine fed.

#### 3.2 Electrode and Energy consumption

The overall consumption of the graphite electrode during the test campaign was calculated as 3.7 kg/MWh. This includes all periods and when certain stable periods are isolated, a much lower number of 2.3 kg/MWh is achieved.

Energy consumption numbers from the stable periods of the demonstration test (Table 7) have been used in a thermochemical model[15] to determine what the energy requirement would be, had the calcine and flux material been fed hot at 900°C. The results from this modelling for both ‘cold feed’ and hot (calcine and flux preheated to 900°), are given in Figure 7. The numbers obtained from the model are the total specific energy

required for smelting the calcine types at the operating conditions indicated. These theoretical numbers are the energy requirements for the smelting process only, i.e. they exclude any heat losses from the smelting vessel's roof, sidewalls and hearth.

Total heat losses during operation was approximately 450 kW at total power input of 1.3 MW. The water-cooled copper panels, water cooled upper sidewalls and roof constituted about 95% of these losses. Furthermore, the heat loss ratio between the lower sidewalls (watercooled copper panels) and the roof plus upper sidewalls ranged between 40 and 60%, subject to whether the electrodes were run in submerged or short arc mode. In the short arc mode the heat losses to the lower sidewalls were lower. The watercooling of both the lower and upper sidewalls ensured that the furnace integrity was protected, with a slag "freeze lining" in the lower sidewall area.

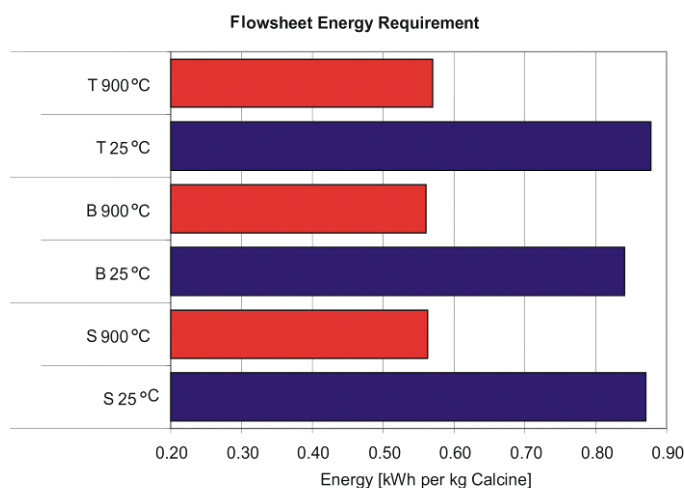


Figure 7: Theoretical energy requirements for smelting 'S', 'T', and 'B' types of calcine - cold and preheated calcine (fluxed)

### 3.3 Alloy Grade

The analyses of the crude ferronickel alloy on a weighted average basis for the three main smelting conditions are given in Table 8.

**Table 8: Crude ferronickel alloy analyses during smelting of 'S', 'T', and 'B' calcine respectively**

Weighted average chemical analyses, mass %	Calcine 'S'	Calcine 'T'	Calcine 'B'
Number of crude ferronickel alloy taps within condition	13	11	8
Silicon	0.13	0.12	0.47
Chromium	0.14	0.21	0.59
Manganese	0.04	0.04	0.05
Iron	77.9	78.0	82.8
Cobalt	2.1	1.3	0.6
Nickel	19.3	19.9	15.1
Copper	0.033	0.025	0.024
Carbon	0.11	0.15	0.45
Sulphur	0.14	0.11	0.08
Phosphorous	0.24	0.24	0.24

The levels of nickel, silicon and carbon in the tapped crude alloy over the duration of the demonstration campaign are shown in Figure 8. Figure 9 depicts the variation of cobalt in the tapped alloy over the campaign duration.

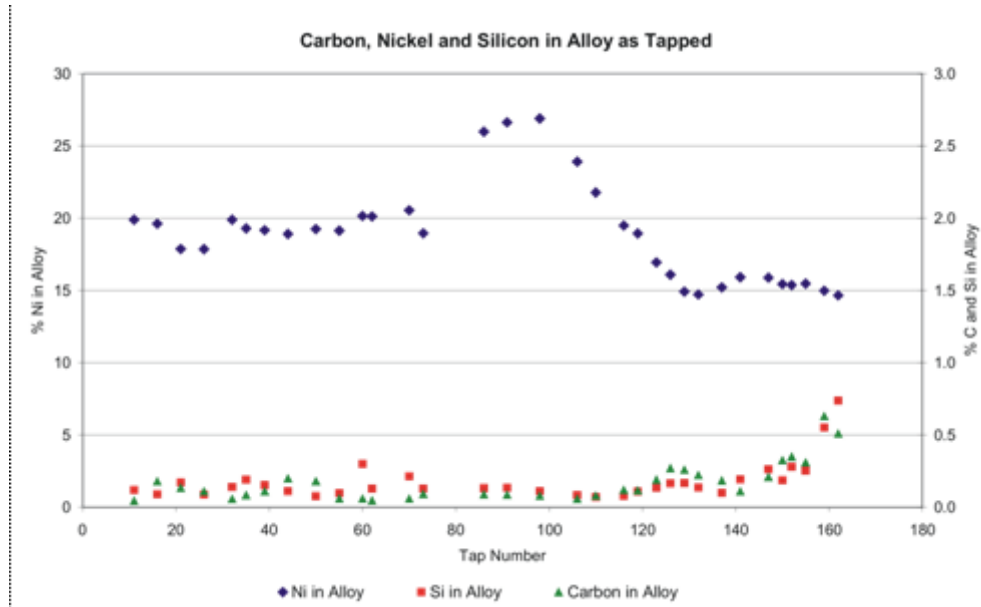


Figure 8: Ni, Si, and C in crude FeNi alloy over the duration of the campaign

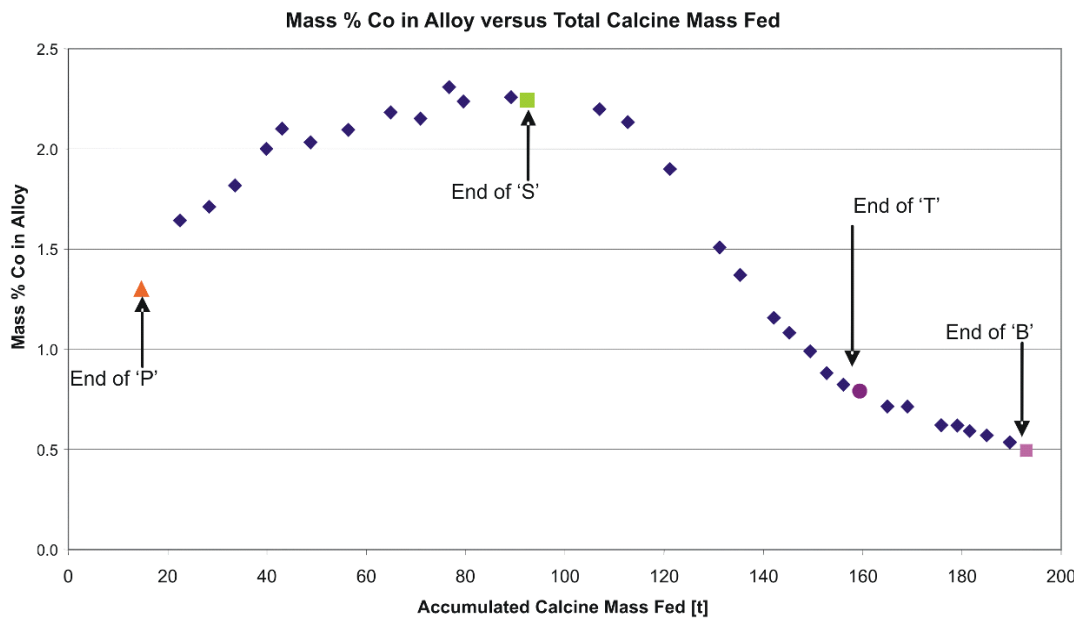


Figure 9: Cobalt crude FeNi alloy over the duration of the campaign

The high initial cobalt levels in the produced alloy are a direct result of the high levels of this element in the 'S' type calcine. The ratio of nickel to cobalt in the calcine is 7.5:1 in the 'S' calcine and increases to 9.3 in the alloy. Under the highly reducing conditions that were employed, it is expected that this ratio in the alloy will closely relate to the ratio between these elements in the calcine feed. For the 'B' type calcine, the Ni:Co ratio was 32:1 in the feed calcine.

#### 4. DISCUSSION OF RESULTS

A main objective of the testwork was to demonstrate that an alloy containing about 20% nickel could be produced at a 90% recovery of nickel. This was obtained during the warm up ('P' – condition) and the 'S' smelting period but not when smelting 'T' or 'B' calcine. The grade-recovery relationships for smelting 'S', 'T', and 'B' are shown in Figure 10. The 'P' condition is not shown, as the instantaneous alloy grade that was produced had to be inferred from the slag analyses. Here it is clear that the recovery was in excess of 90% as the nickel in the calcine was 1.46 % as compared to 0.12% in the discard slag and 13.3 ton slag was produced from 14.7 ton calcine. The inferred nickel in the alloy produced was 33%. The actual grade of nickel in the alloy was lower as the original 480 kg of startup scrap contained only about 10% nickel and had to be

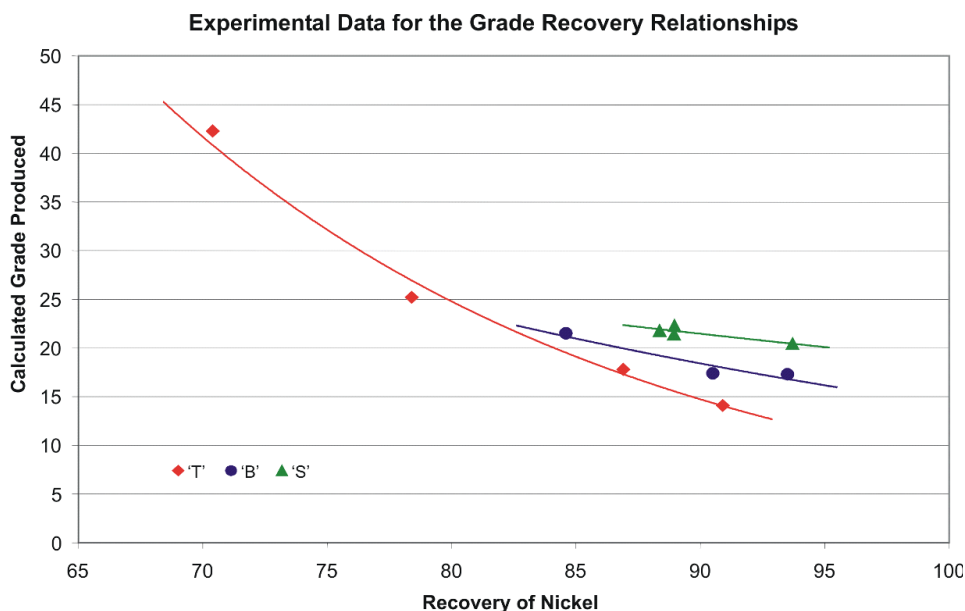
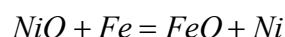


Figure 10: Grade-recovery relationship during smelting of 'S', 'T', and 'B' calcine

concentrated to around 20% during the smelting of the warm up ('P') calcine.

Efforts were concentrated during the smelting of the 'T' and 'B' calcine to achieve 90% recovery even if it meant that grade was not attained. Figure 11 shows how the increase in reductant lowered the nickel content in the resultant alloy, as reductant addition was increased to get to the 90% recovery target.

A thermodynamic evaluation shows that it is theoretically possible to achieve >90% recovery and have at least 20% nickel in alloy when smelting any of the calcine types. Figure 12 depicts results from an equilibrium model for the liquid reaction between slag and alloy.



From this reaction the relationship between nickel and iron recovery can be derived, similarly to what was done by Jones et al[16] for cobalt and iron. The equation that can be derived is given below

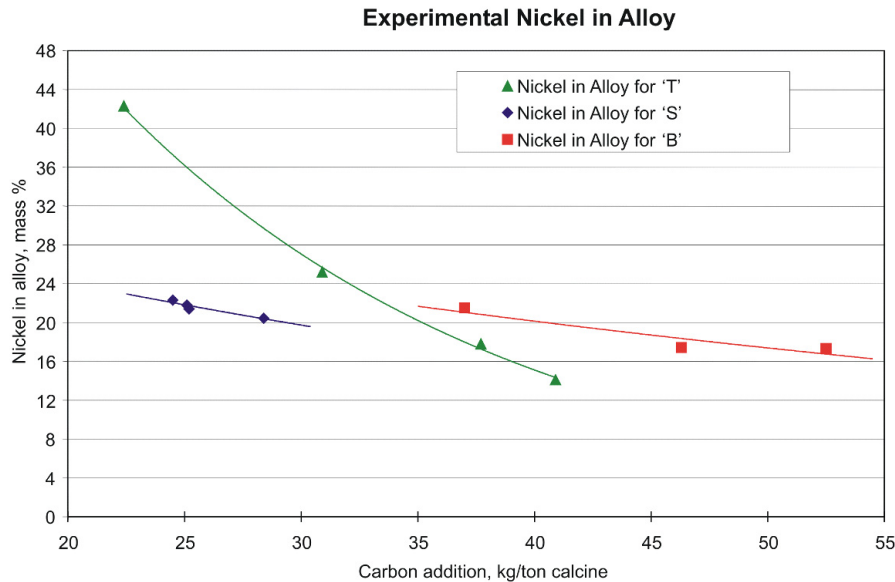


Figure 11: Alloy grade as a function of carbon (in reductant) addition

$$R_{Ni} = K\gamma \cdot R_{Fe} / (1 - \{1 - K\gamma\} \cdot R_{Fe})$$

where:  $K\gamma$  is the equilibrium constant;  $R_X$  = recovery of X, where X = Ni or Fe

The equilibrium constant,  $K\lambda$ , has been obtained for the above reaction from theoretical data[15] and has a value of approximately 160. The data from the demonstration campaign has been superimposed on the graph for the smelting of 'S', 'T', and 'B' respectively. In addition, a curve has been fitted for the actual data, using a value of 20 for  $K\lambda$ .

The reason for not achieving the equilibrium conditions as described above is attributed to the presence of a crusty layer of feed on the surface of the molten bath during smelting. This crusty layer would have inhibited the rate at which fresh calcine assimilates into the bath and reacts with the coal. The reasons for the presence of the crusty layer would have been due to a combination of a number of factors, amongst others;

- Some of the calcine was only partially calcined and the remaining crystalline water would be driven off when the calcine hits the bath surface. The reaction by which the crystalline water is removed is highly endothermic and would cause localized cooling of the bath surface.
- The calcine and resultant slag is highly siliceous and would have had a high viscosity and electrical resistivity. Fluxing with dolime lowers both properties, but for economical reasons, the degree of fluxing needs to be limited as far as possible.
- At the pilot plant scale of operation the ratio of voltage-to-current required is much higher than would be the case for an industrial furnace. The voltage is required to have the electrode clear of the bath, and at the pilot scale, this voltage was of the order of 400V. A consequence of the high voltage required was that at the prescribed power levels, the total current was fixed at between 3 and 4 kA. As arc stability is an issue at low currents, it became an issue, especially for the arc that was closest to the feed entry point.

In fact, the selection of the twin-electrode mode of operation for the demonstration scale testwork, exacerbated arc stability issues as the total current was now split between two arcs, viz. 1.5 to 2 kA per cathode. (With a large industrial furnace, the currents utilized would be an order of magnitude higher, eliminating arc stability issues. Also, the twin cathode configuration could become important if the furnaces were to be scaled significantly above about 50MW, due to the maximum available diameter for graphite electrodes and the limits on current carrying capacity[17]).

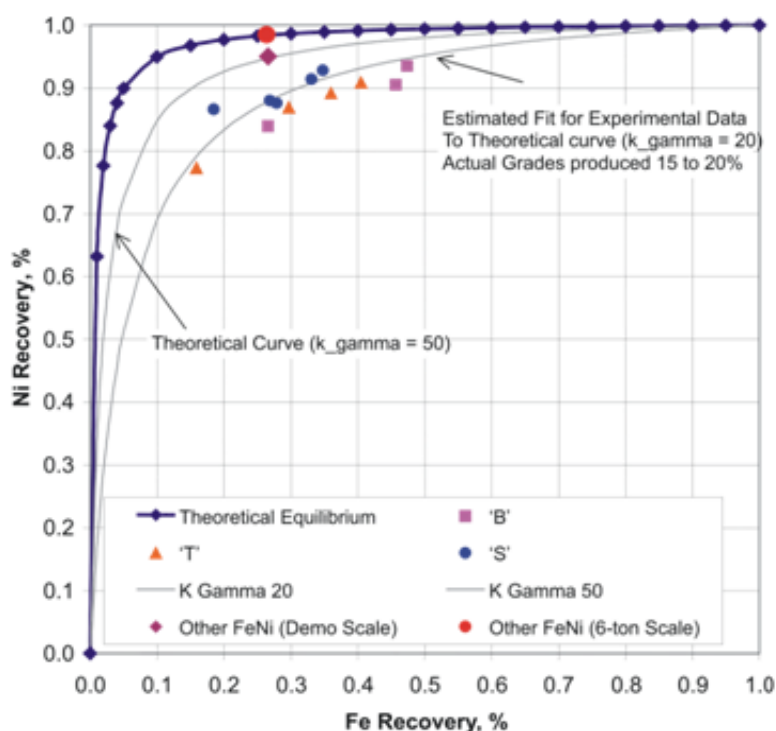


Figure 12: Nickel and iron recovery relationship - theoretical and actual

During the testwork, the operators were limited in their options to improve the bath conditions and attain closer-to-equilibrium smelting. Recalcining to lower the LOI in the calcine was not an option due to time constraints. Temperature was a parameter that was used to some degree to lower the viscosity of the slag. Figure 14 depicts slag viscosity as a function of different temperatures and slag composition in terms of its Fe/SiO<sub>2</sub> ratio. However, at temperatures above 1700°C and where the slag's Fe/SiO<sub>2</sub> ratio is above 0.2, there was a negligible effect on the viscosity and there would be little incentive to operate above this temperature, also for economical reasons. Viscosities were calculated using the model of Urbain[18].

Slag viscosity and resistivity is a strong function of slag composition as shown in Figure 14. Here slag viscosity and resistivities at a fixed temperature of 1700°C were plotted versus the Fe/SiO<sub>2</sub> ratio in the slag. In fact, for the transition type laterite ores, the use of the Fe/SiO<sub>2</sub> ratio in the slag may be more useful for design purposes than the more conventional SiO<sub>2</sub>/MgO ratio.

The correlation by Jiao and Themelis[19] has been used to predict the slag resistivities.

## 5. CONCLUSIONS

The demonstration campaign has shown that highly siliceous low-grade nickel ore from Kazakhstan can be successfully processed in a DC arc furnace. Typical grades of crude ferronickel containing close to 20% nick-

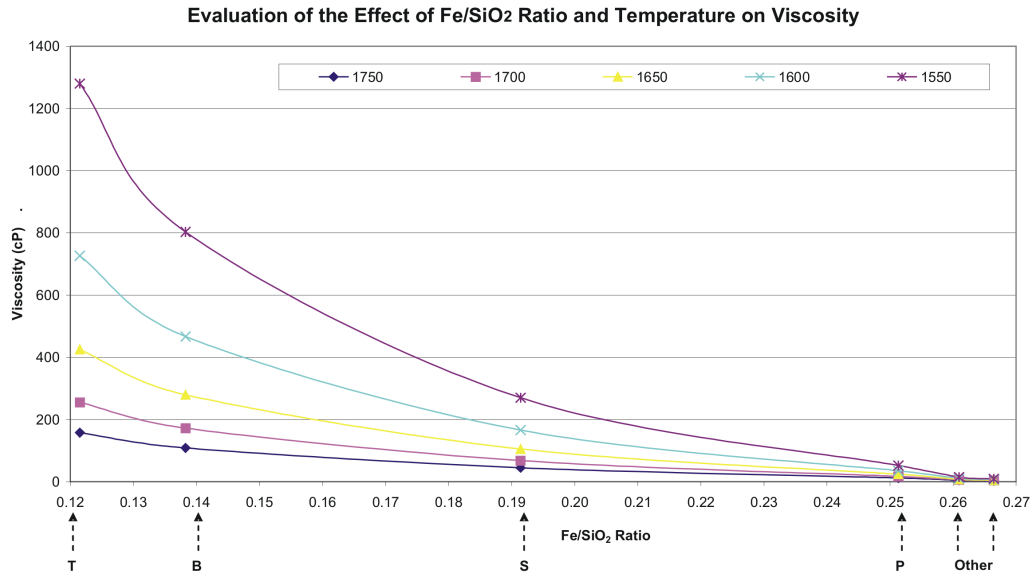


Figure 13: Slag viscosity as a function of Fe/SiO<sub>2</sub> ratio and temperature

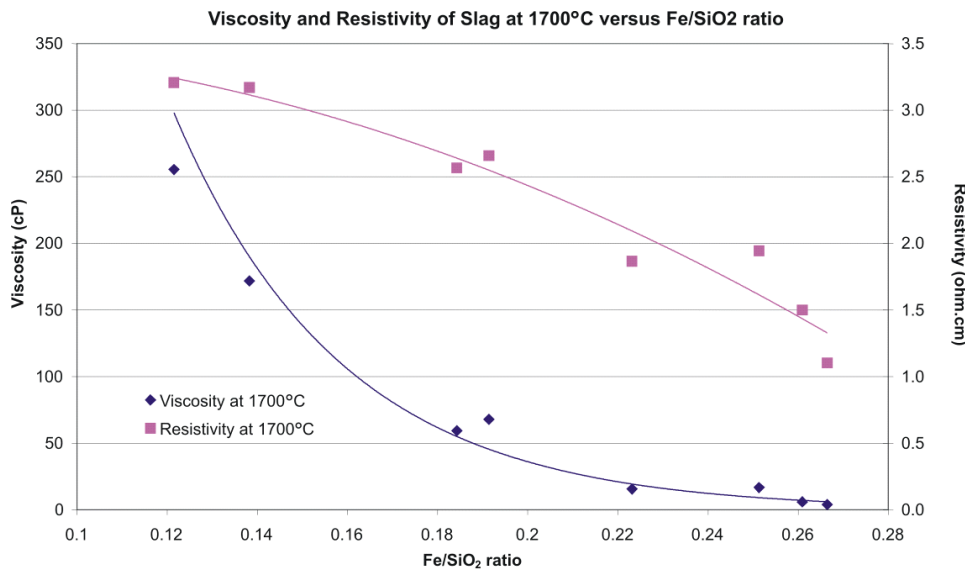


Figure 14: Viscosity and resistivity of slags at 1700 °C as a function of slag Fe/SiO<sub>2</sub> ratio

el could be produced with the higher-grade ore sample. With the lower grade ore samples, the crude ferronickel grades varied between 14 and 20% with the lower end of this range coinciding with higher amounts of reductant to achieve 90% nickel recovery, as calculated based on losses to the slag. The use of watercooled copper panels in the lower sidewalls ensured smelting vessel integrity during the smelting of these highly siliceous ores and resultant aggressive discard slags. Water cooling of the refractory-lined steel shell was used in the upper sidewalls areas and no erosion of these refractories occurred.

To facilitate optimized smelting conditions, to produce a crude alloy with about 20% nickel at nickel recoveries in excess of 90%, it would be necessary to optimize the ore blend and flux addition sensibly. Geological surveys subsequent to the demonstration testwork have shown that the ore reserve contains limonite, nontronite and sapolite in ratios somewhat different than first estimated, and an ore blend will generally be significantly lower in silica than the three samples that were tested during the demonstration campaign. Modelling has shown that an ore blend would require fluxing of only 5%, as opposed to 10 % originally envisaged. The most recent survey also indicates that the 'S' sample was uncharacteristic with respect to its cobalt content. The ore blend envisaged for this project will thus produce ferronickel with improved nickel-to-cobalt ratios.

Larger commercial-scale smelting would have more freedom with respect to operating voltage (whilst maintaining a stable open arc) which will improve the smelting bath conditions and thereby approach equilibrium conditions more closely. This will improve the attainment of a 20% alloy at >90% nickel recovery. The testwork results provide an excellent reference point for a commercial design and the results from the evaluation of viscosity, resistivity and operational stability, will ensure that a robust and flexible process design can be implemented.

## 6. ACKNOWLEDGEMENTS

Mintek would like to thank the sponsors of the demonstration test, Oriel Resources, for permission to publish this paper, and also Bateman BV for their inputs regarding the furnace design.

## REFERENCES

- [1] Bolt, J.R. and Queneau, P., "The Winning of Nickel", Longmans Canada Ltd. Toronto, 1967, pp. 387-453.
- [2] Dalvi, A.D. (Dr), Bacon, W. (Dr), and Osborne, R.C. "The Past and Future of Nickel Laterites", PDAC 2004 International Convention, Trade Show & Investors Exchange, 7-10 March 2004, pp. 1-27.
- [3] Ullman's Encyclopedia, "Nickel", Vol. A17, p. 162.
- [4] Slag Atlas, 2<sup>nd</sup> Edition, Stahleisen, 1995, p. 144.
- [5] Warner, A.E.M., et al. "JOM World Non-Ferrous Smelter Survey, Part III: Nickel Laterite", JOM, April 2006, pp. 11-20.
- [6] Bergman, R.A., "The production of Ferronickel from laterite ores", Fundamentals of Metallurgical Processing, James M. Toguri Symposium, Published by The Metallurgical Society of The Canadian Institute of Mining, Metallurgy and Petroleum, pp. 527-543.
- [7] Diaz, C.M., et al, "A Review of Nickel Pyrometallurgical Operations", Extractive Metallurgy of Nickel and Cobalt, (Edited by G.P. Tyröler and C.A. Landolt, TMS, 1988, Proceedings of the Symposium sponsored by the CuNiCo and Non-Ferrous Pyromet Committee of The Metallurgical Society, 117<sup>th</sup> TMS Annual Meeting, Phoenix, Arizona, 25 to 28 January, 1988.
- [8] Kyle, J.H., "Pressure acid Leaching of Australian Nickel/Cobalt Laterites", Nickel '96 - Mineral to Market, Kalgoorlie, Western Australia, 27 to 29 November 1996, Published by The Australian Institute of Mining and Metallurgy, p. 245.
- [9] Rodriguez, R. I., "Reduction in Energy Cost in Cuban Caron Process Plants", International Nickel Laterite Symposium – 2004, Process and Operational Lessons Learned Part 1, TMS (The Minerals, Metals & Materials Society), 2004, proceedings of Symposium held during the 2004 TMS Annual Meeting in Charlotte, North Carolina, U.S.A., 14 to 18 March, 2004. Edited by W.P. Imrie and D.M. Lane, pp. 657-664.
- [10] Mehmetaj, B and Boom, R., "Ferronickel production in Kosova - Past Performance and New Opportunities", Process Metallurgy, Steel Research 72 (2001), No. 11 + 12, pp. 428-433.
- [11] Slag Atlas, 2<sup>nd</sup> Edition, Stahleisen, 1995, p. 142.
- [12] Lagendijk, H. and Jones, R.J., "Production of Ferronickel from Nickel Laterites in a DC-Arc Furnace", Nickel/Cobalt '97. 36th Annual Conference of Metallurgists, Sudbury, August 1997 or <http://www.mintek.co.za/Pyromet/Laterite/Laterite.htm>.
- [13] Kotzé, I.J., "Pilot Plant Production of Ferronickel from Nickel Oxide Ores and Dusts in a DC Arc Furnace", Presented at Pyromet 2002, Cape Town, South Africa, March 2002, Minerals Engineering 15 (2002) pp. 1017-1022. Also available online at [www.sciencedirect.com](http://www.sciencedirect.com) or [www.elsevier.com/locate/mineng](http://www.elsevier.com/locate/mineng).

- [14] King, M. G., Grund, G. and Schonewille, R., "A Mid-term Report on Falconbridge's 15 Year Technology Plan for Nickel", Proceedings of EMC (European Metallurgical Conference) 2005, 18 to 21 September 2005, Dresden, Germany, pp. 935-954.
- [15] FactSage 5.3.1, Thermochemical Software for Windows, [www.FactSage.com](http://www.FactSage.com).
- [16] Jones, R.T., et al, "Recovery of Cobalt from Slag in a DC Arc Furnace at Chambishi, Zambia", Cobalt Nickel Copper and Zinc Conference, held 16 to 18 July 2001, Victoria Falls, Zimbabwe. Also at <http://www.mintek.co.za/Pyromet/Chambishi/Chambishi.htm>.
- [17] Reynolds, Q.G., and Jones, R.T., "Twin-Electrode DC Smelting Furnaces – Theory and Photographic Testwork", Presented at Pyromet 2005, Cape Town, South Africa, March 2005, Minerals Engineering 19 (2006) pp. 325-333. Also available online at [www.sciencedirect.com](http://www.sciencedirect.com). or [www.elsevier.com/locate/mineng](http://www.elsevier.com/locate/mineng).
- [18] Mills, K.C., "Viscosities of Molten Slags" – Urbain Correlation, Slag Atlas, 2<sup>nd</sup> Edition, Stahleisen, 1995, pp. 349-354.
- [19] Jiao, Q., and Themelis, N.J. "Correlations of Electrical Conductivity to Slag Composition and Temperature", Metallurgical Transactions B, Volume 19B, February 1988, pp. 133-140.